International Journal of Innovation, Creativity and Change. www.ijicc.net
Volume 15, Issue 7, 2021

Bituminous Coal as Anodes for Lithium-Ion Battery (LIBs)

Faisal Muhamdsyah[a], Ahmad Helman Hamdani[b]*, Agung Mulyo[c], [a,,b.,c]Faculty of Geology, Universitas Padjadjaran, Jl. Raya Bandung Sumedang Km. 21, Jatinangor, Sumedang, Indonesia 45363, Email: [a]faizal.muhamadsyah@unpad.ac.id [b*]ahmad.helman@unpad.ac.id, [c]agung.mulyo@unpad.ac.id.

Portable electronic devices and electric vehicles have used lithium-ion batteries (LIB) as a continuous energy storage device. Graphite is one of the anode materials in the battery circuit. However, it only has a low carbon energy capacity, around 372 mAh g^{-1}, whereas, the need for types of devices with large storage capacities will certainly not be fulfilled. The aim of this research is to determine if bituminous coal can be considered a viable alternative to an anode of lithium-ion batteries. Three samples of high volatile bituminous coal from West Java were selected for analysis to determine the electrochemical performance. The coals were acid-washed and carbonized at 800^0 C under nitrogen at 2^0 C min^{-1} for 1 hour. The scanning electron microscopy (SEM), transmission electron microscopy (TEM), and X-ray diffraction (XRD) were used to identify morphology, structural patterns, and pore distribution of coals. Our findings show that coal has small interlayer spacing, is more microporous, and is more ordered. A high reversible capacity of 418 mAh g^{-1} was detected via an electrochemical experiment.

Keywords: *Bituminous Coal, Lithium-Ion Battery, XRD, SEM, TEM*

Introduction

At this time in Indonesia, coal production is mostly used for export to foreign countries; while for domestic use, it is mostly used for electric power generation (PLTU). Down streaming activity in the mining sector is one of the government's efforts to increase the added value of domestic mining products and encourage economic growth. Coal processing in Indonesia have not been optimal in creating added value. Various coal downstream products that have added value, such as gasification products in the form of syngas, Dimethyl Ether (DME) and Lithium batteries (LIBs), can increase state revenue and suppress imports of petrochemical products.

Graphite as a strategic and critical mineral in the US and EU, and in 2020 achieved sales of 4.48 million tons worth $17.56 billion (Emerald Insight, 2015). Graphite was the first to be investigated as an LIB anode considering the thermodynamic stability of the intercalation stage I (KC8) compound and it has a high reversible capacity of 273 mAh g^{-1} at a very small current density of C / 40 (1 C = 279 mAh g^{-1}) (Jian et.al., 2015). Currently, commercial lithium-ion batteries use a lot of graphitic carbon as anode material (Herstedt et al., 2003). Research has proven that graphite has the ability as an excellent intercalation compound for lithium (Park et al., 2013). Graphite has a theoretical specific capacity ranging from 360 -372 mAh g^{-1} (Zhao et al., 2008). It also has good charge-discharge stability so that the battery can be durable and reliable (Zaghib et al., 2003).

The increasing need for graphite supply to meet the increasing demand for Li-ion production cannot be fulfilled due to the limited reserves of natural and synthetic graphite (Olson, et al., 2016; Moores, S. 2016). Many studies have been conducted to find a substitute for graphite as an anode material (Wang et al., 2018; Lu et al., 2018; Varzi et al., 2018); but one that is as good as graphite hasn't been found. Various carbon-based materials are materials that are often used in the Lithium-ion battery industry (Lu et al., 2018; Nitta et al., 2015). In 2016, the use of carbon-based materials as Li-ion anode materials reached 96% of all anode types (Pillot, C., 2017). This is due to the favourable characteristics of making Li-ion anodes; low cost and green environment; as well as better electrochemical performance (Xing et al., 2018; Roberts et al., 2014). Research that has been done shows that in addition to producing heat, coal can also serve as the main material for functional carbon production (Li et al., 2015; John et al., 2019). Several studies of coal-based materials for LIB anodes and sodium-ion batteries have been published (Xing et al., 2018; Gao et al., 2018).

Based on some of the things mentioned above, the research that will be carried out examines coal-based carbon materials for the LIB anode. Three bituminous coals of Bayah Formation were selected as precursors**.**

Research Methodology

Three bituminous coals were selected from the Bayah open-cast mine located in Bayah District, Banten Province. The ASTM International Standard is used in sampling, bagging and preparation for chemical analysis, both proximate and ultimate. To obtain the same size, the coal samples were crushed in a ball mill for 10 minutes and sieved to a size of 200 mesh.

Proximate and ultimate analyses

The coals characteristics were determined by proximate and ultimate analysis based on the ASTM International Standard (ASTM). Three coals from Bayah Formation, West Java were used for the study; the samples were denoted as, B102- raw, B104- raw, and B106- raw.

In the demineralisation method by acid-washing, mineral matter is removed. About 1 gram of coal was mixed with a mixture of HNO_3, HCl, HF in the ratio of 3: 1: 1 respectively at 60^0 C. After one day, the sample was filtered and washed with demineralised water and followed by drying with a temperature of 800 within 12 hours. The samples were named: B102-adm, B104-adm, and B106-adm. Subsequently, the proximate and ultimate examinations are carried out (Table 1).

After the demineralisation process with acid washing is complete, the carbonisation process is carried out at a temperature of 800^0 C for under nitrogen at 2^0 C min-1 within 1 hour, the obtained sample was named, B102-crb, B104-crb, and B106-crb. The proximate and ultimate of original coals, demineralized coal and combustion coal are shown in Table 1.

X-Ray Diffraction (XRD) analysis

The coal structure and main crystalline phases of the coal were analysed by XRD. A fine sample of 0.3 g was dried in an oven at 100^0 C for 12 hours to remove adsorbed water. Then the sample is compressed into rectangular aluminium sample holders and clamped to the sample instrument holder. A Rigaku Miniflex X-ray diffractometer (XRD) with a Cu Kα radiation source (40Kv,40mA) was used for obtaining diffractograms. The sample scanning is carried out in increments from 5^0 to 85^0 (2θ) at intervals of 0.02 and counted for 0.5 sec per step. Bragg's and Scherrer's empirical equation is used to calculate the average carbon crystallite lattice parameters, including height of crystallite (Lc), diameter of crystallite (La), interlayer spacing, and average number of aromatic layers per carbon crystallite (Okolo et al., 2015; Roberts et al .,2015)

$$d_{002} = \frac{\lambda}{2 \sin \theta\ 002} \quad (1)$$

$$L_c = \frac{K\lambda}{\beta 002\ cos\theta\ 002} \quad (2)$$

$$L_a = \frac{K\lambda}{\beta 10\ cos\theta\ 10} \quad (3)$$

$$\text{Nave} = \frac{Lc}{d002} + 1 \quad (4)$$

Where:

λ	the wavelength radiation use (for copper Kα radiation; λ= 1.54056 Å)	$\beta_{002,\ 10}$	the full widths at half maximum of the (002) and (10) peaks
$\theta_{002,}$ 10	peak positions of the (002) and (10) band (^{0})	K	a constant (0.89 for the (002) band and 1.84 for the (10) band).

X-Ray Fluorescence (XRF) analyses

The chemical composition of the coals was identified by using XRF. The concentration of each element was in weight % (wt.%). The NEX DE Energy Dispersive X-ray Fluorescence Spectrometer was used to measure the elemental composition. A powdered sample was placed on the sample holder without an additional matrix.

Scanning electron microscope (SEM)

The morphology and microstructure of the coals were identified via SEM analysis by a SU3500 Hitachi equipment.

Transmission Electron Microscopy (TEM)

Morphology of coal-based carbons was determined by a TEM HT7700 200Kv. A sample of 1 gram of fine coal is placed in a small cone and ethanol is added to be used as a solution medium. Furthermore, the sample was placed in a centrifuge for 5 minutes. The solution was dropped on a copper plate with filter paper. To dry it up, a hot lamp light was directed at the plate

Electrochemical Measurements

Electrochemical Impedance Spectroscopy (EIS)

An EIS is a method for analysing an electrode against a signal alternating current (AC) potential at a lower amplitude (~ 10 mV) of the range of very wide frequency. AC impedance spectroscopy is a very good technique for determining if the kinetic parameters of the electrode process' include electrolytes, layer passivation, charge transfer, and Li+ diffusion.

Cyclic Voltammetry (CV)

The Cyclic Voltammetry (CV) test aims to know the electrochemical performance of the battery that has been made, that is, seen from the intercalation / deintercalation process of lithium ions. This test uses the Automatic Battery Cycler Won A Tech with a voltage range of 0.01 - 3 V and a scan rate 0.1 mV/s.

Charge- Discharge

The galvanostatic charge/discharge tests (CD) used Automatic Battery Cycler Won ATech with a voltage range between 0.01-3V. The CD is used to find out the capability of a material to store energy.

Results

Proximate and Ultimate Analysis

Proximate analysis to determine the content of moisture, ash, volatile matter and fixed carbon has been carried out on a total of 3 coal samples from open pit mining in Bayah Ares, West Java. Standard analysis using ASTM (American Society Testing and Materials) was carried out. The results of the proximate measurement can be seen in Table 1. In addition, measurements of total sulphur and calorific value were carried out (Table 1).

Table 1. Proximate Analysis of coals from Bayah Formation

Coal ID	Proximate Analysis				Ultimate Analysis					Calorific value
	M	Ash	VM	FC	C	H	N	0	S	
	(ad)	(db)	(daf)	(daf)	(ad)	(ad)	(ad)	(ad)	(ad)	(Btu/Lb)
B102-raw	3.15	5.38	38.72	52.75	78.91	6.38	1.49	11.9	1.32	14057
B102-adm	2.68	0.97	31.36	64.99	82.86	4.34	1.21	11.42	0.20	
B102-crb	1.52	0.81	30.12	67.55	84.14	3.82	1.10	10.49	0.18	
B104-raw	2.6	2.57	41.08	53.75	75.85	6.76	1.55	15.3	0.54	14081
B104-adm	2.21	0.96	33.27	64.96	81.16	4.19	1.26	13.49	0.20	
B104-crb	2.02	0.82	30.52	66.64	88.01	3.89	1.02	10.88	0.14	
B106-raw	3.74	2.33	39.34	54.59	72.15	5.02	0.99	20.83	1.01	14299
B106-adm	3.18	0.28	31.87	64.68	81.53	3.46	0.80	14.20	0.18	
B106-crb	2.81	0.16	29.81	67.22	85.11	3.11	0.56	13.03	0.16	

Remark

TM	: Total Moisture	VM	: Volatile Matter
M	: Moisture	FC	: Fixed Carbon
Ash	: Mineral	ad	: Air dry
TS	: Total Sulphur	daf	: Dry ash free
C	: Carbon	db	: Dry base
N	: Nitrogen	H	: Hydrogen
S	: Sulphur	O	: Oxygen

XRF Analysis of Thermal Treatment of the Coals

The XRF research is carried out to determine the mineral matter contained in coal. The results showed that the mineral matter consisted of Al, Si, Fe, Ca, Mg, C and O (Table 2).

Table 2. Elemental composition of coal samples

No.	Sample ID	Si	Al	*Fe*	Ca	Mg	C	O
1	$B104_{crb}$	1.08	0.5	1.4	2.1	0.7	88.4	5.62
2	$B106_{crb}$	2.1	0.8	1.2	2.6	0.9	85.4	6.67

XRD Analysis of Thermal Treatment of the Coals

Figure 1 shows the XRD profile of a coal sample, which shows the characteristics of the diffraction peak of coal: 20^0–30^0 theta (002 peaks) which is less similar from each of the coal samples.

Figure 1. XRD pattern of the Lignite coal and Bituminous coal

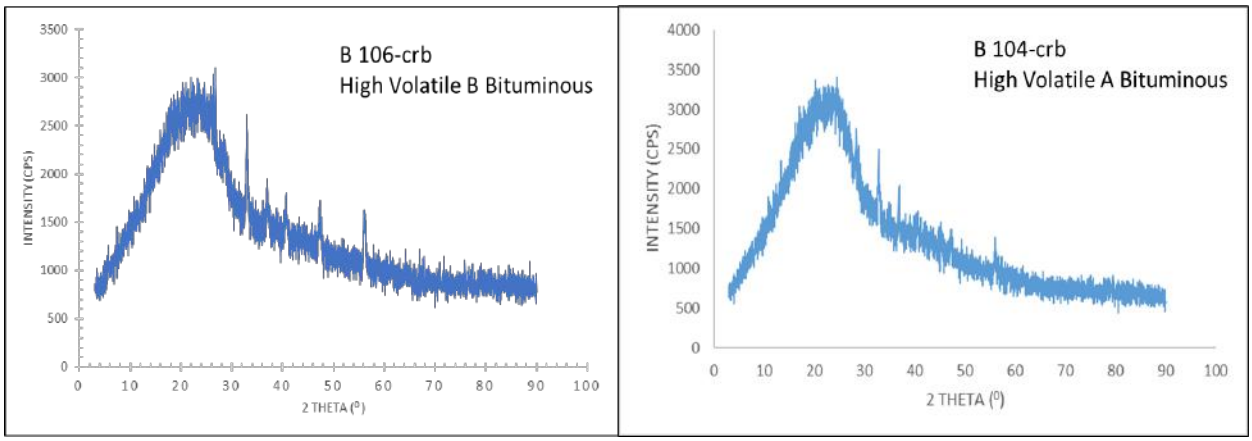

The coals are characterised by having a high diffraction peak (002) and narrowed diffraction peaks (002). Calculation of the interlayer spacings of carbon hexagons *(d002)* of each coal was also relatively similar (Table 3).

Table 3. XRD structural parameters of the coal's thermal treatment at nitrogen 800^0 C

No.	Sample ID	$2\theta_{002}$ (^{0})	$2\theta_{100}$ (^{0})	d_{002} (nm)	Lc (nm)	La (nm)	N*ave*
2	$B104_{crb}$	38.72	45.57	0,356	1.6912	3.0618	5.75
3	$B106_{crb}$	38.61	46.75	0.352	1.8781	2.9812	6.33

Remark

$2\theta_{002}$ (^{0})	: Diffraction carbon layer 002 planes	d_{002} (nm)	: Interlayer spacing
$2\theta_{100}$(^{0})	: Diffraction carbon layer 102 planes	Lc (nm)	: Crystallite height
La (nm)	: Crystallite diameter	N_{ave}	:Average number of aromatic layers

Coal Structure and Morphology

Scanning Electron Microscope (SEM)

Analysis of the coal structure and morphology using SEM (scanning electron microscope) and TEM (transmission electron microscopy) has been done. From the SEM interpretation, it is found that the particle size of the two coal samples shows a predominance of sizes ranging from 0.5-1 µm (Figure 2). A particle size smaller than 4 µm will provide powerful electrochemical analysis results. Both coal samples show relatively homogeneous small size

mineral crystals. The presence of minerals in the coal matrix can be seen by the degree of brightness (luminous). The brighter level indicates the element content of Al, K, Si and Na. Meanwhile, the darker colour indicates the element content of the chalcophile group.

Figure 2. SEM picture of coal samples (Upper part). Histogram of particle size distributions of coals (Lower part). Line **A-A1** and Line **B-B1** are indicated micro-fissure. **P** indicates a micropores

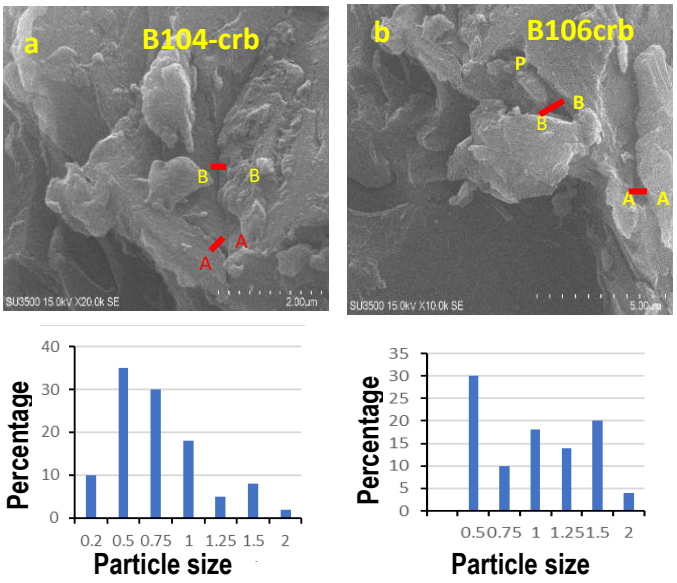

The micro-fissures and micro-pores of coal samples B 104-crb and B 106-crb have been determined by SEM analysis. The B-104-crb has a micro-fissure aperture smaller than in B-06-crb) are 0.25 nm and 0.55 nm, respectively. The coal sample of B 106-crb is more porous than B 104-crb.

Transmission Electron Microscopy (TEM)

Transmission Electron Microscopy (TEM) is another tool used to identify the structural features of the coals (Das et. al.,2016). Das et all (2016) states that the nanoscale material will be found in the form of a hollow carbon sphere together with carbon groups. The typical image of a carbon nano tube (CNTs) is shown in Figure 3. The diameters of the CNTs are in the range of 16.27–31.43nm. The presence of iron nano material was also identified as black spots in Figure 3.

Figure 3. Image of TEM of carbon nano tube (CNTs)

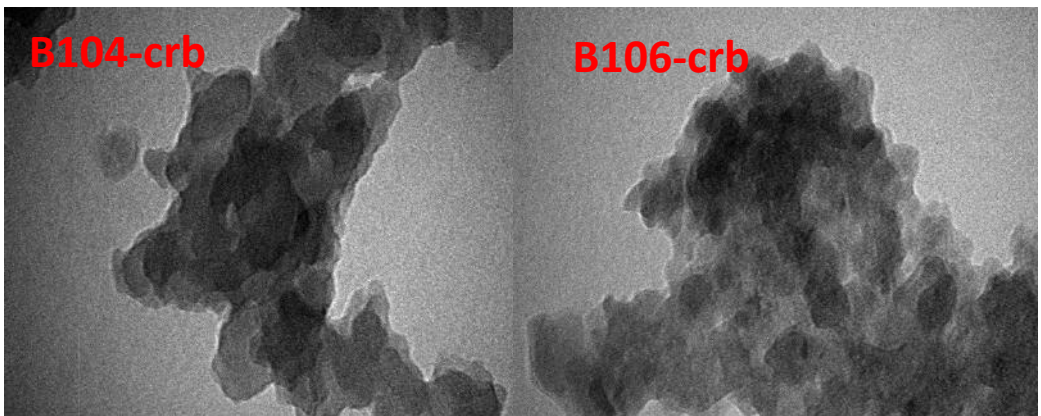

Result of Electrochemical Measurements in LIBs

Cyclic Voltametry (CV)

Cyclic voltammetry (CV) measurements were carried out on bituminous coal samples that had undergone carbonisation at a temperature of 800^0 C in inert nitrogen gas (thermally treated bituminous coal) as seen in Figure 4.

Figure 4. Cycle Voltammogram of thermally treated bituminous coal (B 104 CRB)

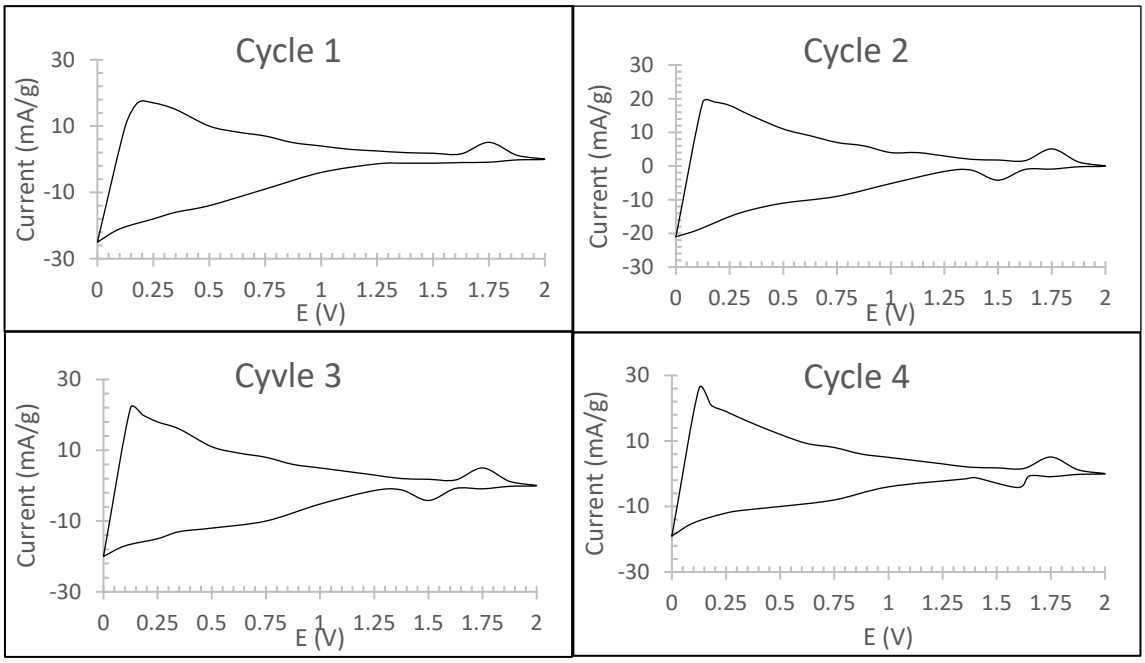

Cyclic Voltametry (CV) testing aims to determine the electrochemical performance of the battery, which is seen from the lithium ion intercalation/deintercalation process. The redox peaks are related to the process intercalation (reduction) and deintercalation (oxidation) of lithium ions. The first cycle of Cyclic Voltammetry (CVs) tests of combustion treated sample (nitrogen at 800^0 C), indicated irreversible capacity (Figure 4) caused by solid electrolyte interphase (SEI) formation. The 2^{nd} to 4^{th} cycles (Figure 4) were alike with the reversibility capacity. In CVs, the reversibility peak was determined around 1.78 V. In the second cycle, irreversibility was disappeared, due to more stable current deliverance in the subsequent cycle.

Electrochemical Impedance Spectroscopy (EIS) *Testing*

The sample was assembled into a battery of type coin cell and measured the conductivity value and impedance through Electrochemical Impedance Spectroscopy (EIS) at a frequency of 0.5 - 20000 Hz and a voltage 0.1 Volt. This characterisation was carried out by flowing the

alternating current (AC) in the so that the characterisation results form an impedance that changes with the frequency function of a given AC current.

Figure 5. Nyquist plots of treated bituminous coal (B 104 CRB)

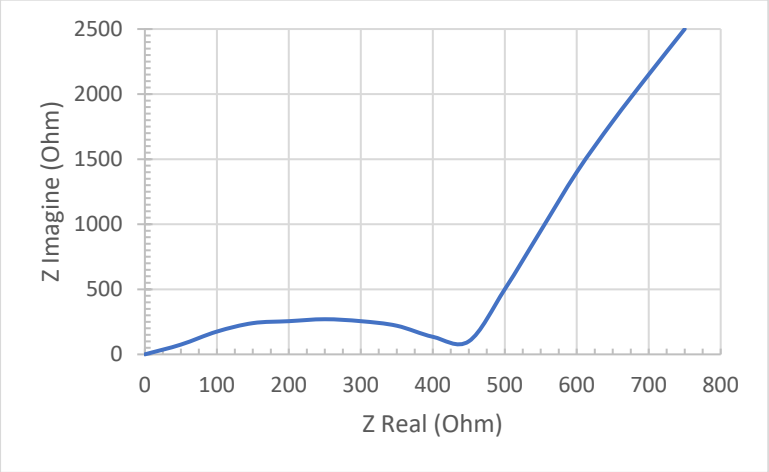

From Figure 5 it can be seen that the battery sample forms a semicircle pattern and straight-line patterns. The semi-circle pattern represents the electrolyte resistance that occurs because the electrochemical reaction in the electrolyte which is deep a certain state between the electrolyte and the surface of the active material. The pattern straight line represents the inward diffusion of lithium ions bulk material electrodes or so-called Warburg diffusion. This pattern shows that the electrodes being made are capable of storing lithium ion so it can be used in lithium-ion batteries. Coal B 104-crb shows the low charge-transfer resistance which represents a high degree of crystallinity, related to the high rank of the coal.

Charge–Discharge Measurement

The results of the charge / discharge test for the thermal treatment of B 104 CRB are shown in Figure 5. The charge-discharge test with this rate of 0.1 C is done to determine the capabilities of the battery inside accepting the loading current.

Figure 6. GCPL profiles of thermally treated bituminous coal B 106 CRB at 800^0 C nitrogen.

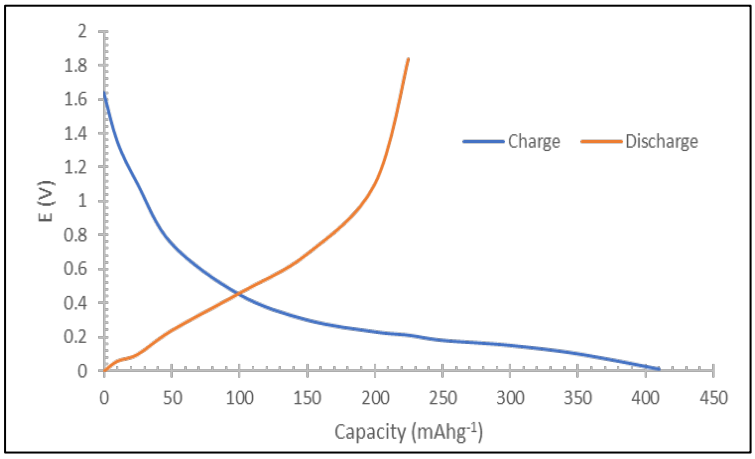

The charge and discharge capacity obtained from coal sample of B 106-crb are 418.4, and 225.3 mAh g^{-1}, respectively. The Initial Coulombic efficiency (ICE) is 53.8%.

Discussion

The proximate and ultimate data of the bituminous are tabulated in Table 1. XRF data was tabulated in Table 2. These coals are characterised by lowest moisture (1.52–3.74 %), and low in ash yield (0.16-5.38 %). The volatile matter (VM) ranges from 29.81% to 38.72% and fixed carbon (FC) from 52.75% to 67.22%. Based on caloric value (ASTM Standard), coals in the research area should be grouped as bituminous type coal. Meanwhile, based on volatile matter content, bituminous coal is categorised as High Volatile A Bituminous (B104) and (2) High Volatile B Bituminous (B102, B106). The process of acid washing and carbonisation (thermal treatment) of coal samples causes detrimental mineral matter to be lost and causes an increase in carbon content; for example, original coal (B 104-raw), acid washing coal (B 104-adm) and carbonisation coal (B 104-cbr) are 75.85%, 81,16% and 88.01%, respectively. Two coal samples; which have the highest content of carbon were selected for XRD, SEM, TEM analysis; i.e, B 104-crb and B 106-crb.

Figure 1 presented the XRD profile of B 104-crb and B 106-crb, shows the characteristics of the coal structure with a peak intensity of 002 which is higher than the other bands (10 peak and 100 peak). The appearance of a clear 002 peak band at ~260, indicated the interlayer spacing of the disordered carbon (crystalline carbon), and 100 peak bands at 420 represent an amorphous phase of carbon. Table 4 lists the XRD data of all the samples (B 104-crb, B 106-crb). The d002 of all coal samples of B 104-crb, B 106-crb is relatively similar at about 0.356 nm, 0.352 nm, respectively. Compared with the d002 value of pure graphite, the d002 of coal value in the study area is greater than the average value of graphite (0.33 nm), indicating that the degree of crystalline is low order. The more interlayered space order should be good for anode materials.

The nanoballs and CNTs of carbon nanostructures can be recognised in coal samples through TEM interpretation. The individual area and size of the nanoballs ranged from 16.27 to 31.43nm. The B 106-raw coal sample has a higher calorific value (14,299 Btu/Lb) than the other coal samples (B 104-crb (14,081Btu /Lb) so that the interlayer spacings of B106-crb are relatively lower than the B 104-crb (Figure 3). Coal B 106-crb has the ability to increase diffusion resistance and rapid intercalation, due to its properties of more ordered lattice-layer microstructure with a specific orientation. During the carbonisation process, there will be volatilisation of small molecules so that a porous structure will be formed and the BET specific surface area of the coal-based carbons will decrease. The micropores were dominated in B 106-cbr. Therefore, in the coal sample of B 106-crb the micropore distribution is greater than in the B 104-crb, so the potential for active storage will be greater at B 106-crb.

The Cycle Voltammogram (CV) curve of 4 cycles of B 106-cbr shown in Figure 4 shows a wide irreversible peak at 1.75 V on the first cycle and illustrates the relationship with the initial SEI formation on the electrode surface. However, in the subsequent cycle this reversible peak was observed and reflects that the SEI has been stably formed in the first cycle. It was also observed that in the following cycles there was overlapping, reflecting the ability of the good reversibility of bituminous coal-based carbon anodes.

Conclusion

The carbonisation process at a temperature of 800^0 C against the raw bituminous coal makes it possible to obtain purer coal for the anode material, reduce ash content, increase fixed carbon and reduce volatile matter. It can also change the original coal structure to be more interlayered spaced, more regular, and more microporous.

The electrochemical performance of carbonised bituminous is showing a positive sign of being developed as a large energy storage area, is characterised by an acceptable initial coulombic efficiency value and high charge capacity (418 mAh g^{-1}). Finally, a new paradigm has been found in this research, related to the potential of bituminous which has undergone a carbonisation process as an anode material in a lithium-ion battery.

Acknowledgements

This research was funded through the Padjadjaran University Research Program in the form of an Academic Leadership Grant (ALG) in 2020. For this, the author would like to thank the Chancellor of Universitas Padjadjaran.

Conflicts of Interest

"The author(s) declare(s) that there are no conflicts of interest regarding the publication of this paper."

REFERENCES

A D. Roberts, Li, X. Zhang, H. (2014). Porous carbon spheres and monoliths: Morphology control, pore size tuning and their applications as Li-ion battery anode materials. *Chem. Soc. Rev*., 43, 4341–4356.

A R. John, Nour A. L, Cecile A L, Moulay T S, Joumana T, Abdelkader O, and Fouad G. (2019). Bituminous Coal as Low-Cost Anode Materials for Sodium- Ion and Lithium-Ion Batteries. *Energy Technol*ogy, 7, 1900005. 1-14

A. Varzi, Mattarozzi, L. Cattarin, S. Guerriero, P. Passerini, S. (2018). Batteries: 3D Porous Cu–Zn Alloys as AlternativeAnode Materials for Li-Ion Batteries with Superior Low T Performance. *Adv. Energy Mater*., 8, 1701706

B. Xing, Zhang, C. Cao, Y. Huang, G. Liu, Q. Zhang, C. Chen, Z. Yi, G. Chen, L. Yu, J. (2018) Preparation of synthetic graphite from bituminous coal as anode materials for high performance lithium-ion batteries. *Fuel Process. Technol*. 172, 162–171.

C. Li, Yu, C. Hu, W.B. Yang, C.T. Zhao, S. (2017). Conversion of coal into nitrogen-doped carbon dots with singlet oxygen generation and high quantum yield, *Chem. Eng. J*. 320, 570-575

C. Pillot. (2019). The Rechargeable Battery Market and Main Trends 2016-2025. In Proceedings of the 33rd Annual International Battery Seminar & Exhibit, Fort Lauderdale, FL, USA, 20 March 2017. Available online: http://cii-resource.com/cet/FBC-TUT8/Presentations/ Pillot_ Christophe.pdf (accessed on 25 July 2019).

D. W. Olson, Virta R. L., Mahdavi M., Sangine E. S., Fortier, S. M. (2016). Natural graphite demand and supply - Implications for electricvehicle battery requirements. *Spec. Pap. - Geol. Soc. Am*. 520, 67−77

Emerald Insight. (2015). Global Graphite Market Will Reach US$17.56 billion in Terms of Value and 4.48 Million Tons in Terms of Volume, in 2020. *Anti-Corros. Methods Mater*. 62, 1.

G N Okolo Neomagus H.W, Everson R. C,.(2015). Chemical–structural properties of South African bituminous coals:insights from wide angle XRD–carbon fraction analysis,ATR–FTIR, solid state13CNMR,and HR TEM techniques. *Fuel* (158), 779–792.

H. Zhao, J. Ren, X. He, J. Li, C. Jiang, C. Wan, 2008. Modification of natural graphite for lithium ion batteries *Solid State Sci*., 10(5), 612-617

Iijima, Sumio; Ichihashi, Toshinari (17 June 1993). Single-shell carbon nanotubes of 1-nm diameter. *Nature*. 363 (6430). 603–605.

J. Lu, Chen, Z. Pan, F. Cui, Y. Amine, K. (2018). High-Performance Anode Materials for Rechargeable Lithium-Ion Batteries. *Electrochem. Energy Rev*. 1, 35–53.

J. Park , Park SS, Won YS. (2003). In situ XRD study of the structural changes of graphite anodes mixed with SiOx during lithium insertion and extraction in lithium ion batteries. *Electrochimica Acta*, 107, 467-472.

K. Zaghib, X. Song, A. Guerfi, R. Rioux, K. Kinoshita, (2004), Purification process of natural graphite as anode for Li-ion batteries: Chemical versus thermal, *J. Power Sources*, 119, 8-15.

M. Herstedt, L. Fransson, K. Edström. (2003). Rate capability of natural Swedish graphite as anode material in Li-ion batteries. *Journal of Power Sources*, 124(1), 191-196

M. J**.** Roberts,Everson R C,Neomagus H W,.(2015)**.** Influence of maceral composit**i**on on the structure, properties and behaviour of chars derived from South African coals. *Fuel* 142**.**9–20.

N. Nitta, Wu, F. Lee, J.T. Yushin, G. (2015). Li-ion battery materials: Present and future. *Matter. Today* 18, 252–264

Q. Jiang, Zhang, Z. Yin, S. Guo, Z. Wang, S. Feng, C. (2016). Biomass carbon micro/nano-structures derived from ramie fibers and corncobs as anode materials for lithium-ion and sodium-ion batteries. *Appl. Surf. Sci*. 379, 73–82

S. Gao, Y.K. Tang, L. Wang, L. Liu, Z.P. Sun, S. Wang, et al..(2018) Coal-based hierarchical porous carbon synthesized with a soluble salt self-assembly-assisted method for high performance supercapacitors and Li-ion batteries, *ACS Sustain. Chem. Eng*. 6 (3), 3255-3263.

S. Moores, (2016). Battery grade graphite shortage on horizon as demand rockets. *Benchmark Mineral Intelligence.* 14−16.

S. Wang, He, M. Walter, M.; Krumeich, F.; Kravchyk, K.V.; Kovalenko, M.V. (2018) .Monodisperse CoSn2 and FeSn2 nanocrystals as high-performance anode materials for lithium-ion batteries. *Nanoscale*, 10, 6827–6831.

T Das, B. Saikia, B. Kand (2016) Formation of carbon nano-balls and carbon nano-tubes from northeast Indian Tertiary coal:Value added products from low grade coal. *Gondwana Research* 31, 295–304.